Theor Chim Acta (1989) 76: 33–46

Theoretica Chimica Acta

A CASSCF-CI study of the coordination of ethylene with iron

Per-Olof Widmark and Björn O. Roos
Department of Theoretical Chemistry, Chemical Centre, P.O. Box 124, S-221 00 Lund, Sweden

(Received October 17; revised and accepted December 29, 1988)

Summary. Complete active space SCF, CASSCF, and contracted CI calculations have been performed on the π-bonded complex between ethylene and an iron atom. An extended basis set of the ANO type was used, which included polarization functions on all centers. The results indicate an attractive interaction between Fe $^5F(d^7s)$ and ethylene, with an estimated binding energy of 14 kcal/mol. The low spin complex arising from Fe $^3F(d^7s)$ was found to be bound with 18 kcal/mol. Both these potential minima are, however, above the ground state of the iron atom. It is concluded that the interaction between atomic ground state iron and ethylene is not of the normal π-bonded type, but is dominated by dispersion forces. A preliminary study showed this interaction to be almost isotropic, with no preferred site for the iron atom.

Key words: Iron–ethylene — CASSCF — CI — Transition metal complex

Introduction

Studies of the chemical bond between transition metal atoms and small molecules have in recent years achieved considerable interest, both theoretically and experimentally. Theoretically the use of 'state of the art' *ab initio* quantum chemical methods has in several cases led to a detailed understanding of the bonding mechanism. These calculations have shown that strong coupling between different electronic states of the metal atom is an important factor in the

bond formation. The obvious reason is the near degeneracy occurring between configurations of the type $d^n s^2$, $d^{n+1}s$, and d^{n+2}. It is therefore necessary, even for a qualitative understanding of the bonding, to go beyond the Hartree–Fock level of theory and use a multi-configurational description of the wave function. Most studies of these systems have therefore been made at the MCSCF level of theory. For a quantitative description of structure and binding energies it is necessary to use extended AO basis sets and to include dynamic correlation effects, which is normally done using configuration interaction techniques. Examples of this type of theoretical study of small molecules containing a transition metal atom can be found in [1–8].

One motivation for these studies has been to mimic the chemisorption process on a metal surface by the simple single atom model. Of course the knowledge of these chemical bonds has general importance for our understanding of transition metal chemistry, since they occur on surfaces, in clusters, and in organometallic systems. Recent developments in matrix isolation spectroscopy has made it possible to obtain explicit experimental information on the interaction between isolated transition metal atoms and small molecules as well. Thus a direct comparison between the theoretical results and the experimental findings is possible.

Quantum chemical calculations have been used in the present paper to characterize the bonding between an iron atom and ethylene. Previously, the corresponding nickel–ethylene system has been studied using similar methods [2]. The bonding between the nickel atom in the $^1D(d^9s)$ state and the π system of ethylene was found to follow closely the Dewar–Chatt–Duncanson (DCD) model [9]. The detailed mechanism is, however, intricate and involves considerable mixing of different configurations on nickel. The interaction between d^9s and ethylene is repulsive due to the overlap between the $4s$ orbital and the π orbital on ethylene. This overlap is, however, reduced by an *sd* hybridization in the singlet coupled pair $4s$, $3d\sigma$; at large distances both these orbitals are singly occupied. As the ethylene gets closer, the orbital perpendicular to the NiCC plane increases its occupation while that of the other decreases. The process results in an unshielding of the $3d$ orbitals, and a donation of electrons to the π^* orbital in ethylene occurs, which is balanced by a back donation from the π orbital. The computed binding energy was (in the most extensive calculation) found to be 19.8 kcal/mol. Thus, nickel–ethylene is bound with more than 10 kcal/mol with respect to the nickel atom ground state. On the other hand, the corresponding triplet state was not bound, the reason being that no *sd* hybridization is possible when the $4s$ and $3d$ electrons are triplet coupled. Actually, a weak bond of around 1 kcal/mol was obtained for the nickel–acetylene complex in a similar study [5]. The mechanism here was unshielding due to an *sp* hybridization on the nickel atom.

Can one expect to find the same binding mechanisms in the low and high spin states of the π complex formed between an iron atom and ethylene? The possibility of *sd* hybridization relies on the energy difference between the low spin $d^{n+1}s$, d^{n+2} and $d^n s^2$ configurations. Since the $d^{n+1}s - d^{n+2}$ energy difference is much larger in iron than in nickel one might expect *sd* hybridization to be less

favourable in iron; the energy difference $d^7s - d^6s^2$, on the other hand, is small (around 20 kcal/mol). Also, the d^6sp configuration has a relatively low energy, which might favour a bonding mechanism involving *sp* hybridization in the low spin case. However, the $^3F(d^7s)$ state is located 34 kcal/mol above the $^5D(d^6s^2)$ ground state. The corresponding energy difference in nickel is only 9 kcal/mol. It is therefore rather unlikely that iron–ethylene will have a low spin ground state. A recent CASSCF study of the similarly bound FeCO molecule gave a bonding energy of 29 kcal/mol for the $^3\Sigma^-$ state, which places it 5 kcal/mol above the iron atom ground state [6]. A CIPSI calculation on the same molecule [8] gave the similar bond energy 30 kcal/mol. It is concluded in the paper that FeCO has a low spin ground state, a statement which is not corroborated by the quoted bond energy. Nickel–ethylene has a smaller binding energy than NiCO, and it can be expected that the same is true for the iron complex. The tentative conclusion is that the iron–ethylene complex has a high spin ground state and consequently a small bond energy dominated by dispersion interaction terms. The results of the present investigation are in agreement with this analysis.

Two matrix isolation investigations of iron–ethylene interactions have appeared in the literature [10, 11]. The first of these, a combined IR and Mössbauer study, suggests that the major product at low iron concentrations is FeC_2H_4, in a π-bonded form [10]. Kafafi et al. [11], however, give strong evidence that the complex found by Parker et al. is actually $Fe(C_2H_4)_n$, where n is larger than one. The conclusion is based on a study of the dependence of the IR spectrum on the ethylene concentration. The mono-alkene complex is also found in the investigation of Kafafi et al. [11], but the IR spectrum indicates that the interaction between atomic iron and ethylene is through one or more of its hydrogen atoms, rather than directly with the carbon atoms. The fact that the compound $HFeC_2H_3$ was formed by photoexcitation of the ethylene–iron complex gives further support to such a structure. The same group also studied the interaction between iron and acetylene [12], and again it was concluded that iron binds to one of the hydrogens in the mono-iron adduct.

The present study is mainly concerned with the π-bonded complex. A tentative study of the dispersion interaction in the other conformations shows no preferred binding site for iron. Actually the computed binding energies indicate that the iron atom is only very weakly bound to ethylene, and is almost free to move between different locations.

2. Details of the calculations

2.1. Basis set

The computational procedure used in the present study follows the earlier study of NiC_2H_4 closely, but with one important exception: much bigger AO basis sets were used here. These basis sets were of the ANO type as suggested by Almlöf and Taylor [13]. The primitive set used for iron was based on the 14*s*, 9*p*, 5*d* primitive set of Wachters [14], augmented with one *s*-type, three *p*-type, two

d-type and three *f*-type GTOs. The *s*-, *p*-, and *d*-type functions were chosen as even tempered continuations of the two outermost primitives in Wachters' basis. Exponents of the *f*-type functions were also chosen as even tempered. The scaling factor and largest exponent were optimized by coupled pair functional (CPF) calculations on the $^5D(d^6s^2)$ ground state of the iron atom [15]. This optimization yielded the exponents 5.18, 1.62 and 0.50.

The carbon primitive basis was taken as the van Duijnenveldt 9*s*, 5*p* set [16], augmented with one *s*-type, one *p*-type, and three *d*-type functions chosen in the same way as for iron. The exponents used for the *d*-type functions were: 1.80, 0.60, and 0.20. The basis set for the hydrogen atom was the 6*s* set of van Duijnenveldt augmented with three *p*-type primitives with exponents 2.00, 0.80, and 0.32.

The contracted basis set was obtained using a modification of the ANO scheme suggested by Almlöf and Taylor [13]. CPF calculations were performed for a number of electronic states of each atom, and the atomic natural orbitals (ANOs) were obtained by diagonalizing the average of the first order density matrices obtained in these calculations; the orbitals with the highest occupation numbers were then chosen. For the iron atom, CPF calculations were made on the states Fe $^5D(d^6s^2)$, Fe $^5F(d^7s)$, Fe^+ $^6D(d^6s)$, and Fe^- $^4F(d^7s^2)$, while for carbon, the averaging was performed for the states C $^3P(s^2p^2)$, C^+ $^2P(s^2p)$, and C^- $^4S(s^2p^3)$. The hydrogen ANOs were obtained from calculations on the hydrogen atom, H_2, and H_2^+.

The number of ANOs chosen for the calculations on FeC_2H_4 was 7*s*, 5*p*, 4*d*, 2*f* (large basis) or 6*s*, 4*p*, 3*d* (small basis) for iron, 4*s*, 3*p*, 1*d* for carbon, and 3*s*, 1*p* for hydrogen. The small basis set for iron was used primarily for the low spin triplet state of the complex, for which we were unable to perform CI calculations with the big basis set without truncating the virtual orbital space—a procedure which is not recommended with ANO basis sets. In all calculations the *s*-components of the *d*-type functions and the *p*-components of the *f*-type functions were deleted in order to allow easier analysis of the wave functions.

The iron basis set was tested in a series of SCF, CCI, and CPF calculations on different spectroscopic states of the iron atom and its positive and negative

Table 1. Transition energies in kcal/mol, from the Fe $^5D(d^6s^2)$ ground state

	Primitive set		ANO set			
	SCF	CPF	SCF	CCI	CPF	Exp
Fe $^5F(d^7s)$	41.49	24.89	41.80	24.35	24.68	20.16
Fe $^3F(d^7s)$	—	—	57.15	38.62	—	34.32
Fe $^3F(d^8)$	171.88	107.88	172.09	119.10	108.06	93.96
Fe^+ $^6D(d^6s)$	145.48	175.78	145.59	168.33	175.77	182.20
Fe^- $^4F(d^7s^2)$	48.43	7.85	48.40	18.71	6.92	−10.84
Fe $^7D(d^6sp)$	—	—	27.19	46.58	—	54.96
Fe $^5D(d^6sp)$	—	—	47.90	64.53	—	73.62

ions. Some of the results obtained, using the large basis set, are given in Table 1. As in all studies using ANO type basis sets the contraction error on the calculated energies is negligible. Since configurational mixing is an essential feature in the formation of the iron–ethylene bond, it is important that the method and basis sets used are capable of producing reasonable values for the atomic excitation energies. As can be seen in Table 1 this is not the case for the SCF results, although the correlated methods do give more accurate values.

2.2. The wave function

The complete active space (CAS) SCF method [17, 18] was used as the zeroth level of approximation in the studies of the iron–ethylene π-complex. The active orbital space used in these calculations comprised the iron atom $3d$ and $4s$ orbitals, and the bonding and antibonding orbitals of the C–C bond in ethylene: CCσ, CCσ*, CCπ, and CCπ*.

The CASSCF wave functions include near degeneracy mixing, which is an important feature for the type of bonding occurring in transition metal complexes. Experience from the NiC_2H_4 calculations showed that the *sd* hybridization involved two important configurations [2]. Also, the electron donating bond between $3d_{xz}$ and the π^* orbital of ethylene is weak, and both the bonding and the antibonding orbitals have considerable occupations. An MCSCF type of wave function is thus needed for a proper description of the bonding. However, it is also well known that dynamic correlation effects are mandatory for a quantitative determination of binding energies and other properties of the system. Here we have used the contracted CI (CCI) method to include these effects [19]; the iron $3d$ and $4s$ electrons together with the C–C σ and π electrons were correlated in these calculations. Reference configurations chosen for the multi-reference CI wave functions were obtained as the "SCF" configuration plus configurations corresponding to the following excitations: $(\pi)^2 \rightarrow (\pi^*)^2$, $3d_{xz} \rightarrow \pi^*$, and $(3d_{xz})^2 \rightarrow (\pi^*)^2$. For quintet states this yields four configuration state functions (CSFs), while 12 CSFs are obtained for the triplet state. The details of the reference space is given in Table 2. The nuclear configuration and coordinate system used is shown in Fig. 1. The $3d$ orbitals in Table 2 are quantized along the y axis. Thus $3d\sigma$ is approximately $2y^2 - x^2 - z^2$. With this labelling scheme, the *sd* hybridization occurs between the $4s$ and the $3d\delta$ orbitals. However, no *sd*-mixing takes place in the high spin case, for which both orbitals have the occupation number one in all reference configurations. The number of configurations is three times bigger in the low spin case since the *sd* hybridization here gives rise to three configurations with occupations (2, 0), (1, 1), and (0, 2). The labels used for the orbitals in Table 2 indicate only the major feature. The true orbitals are of course delocalized, with contributions from several atomic orbitals.

The potential curves arising from the $^5D(d^6s^2)$ and $^{3,5}F(d^7s)$ states of the iron atom π bonded to ethylene were examined. All three of these states have components in each of the four representations of the C_{2v} point group of the

Table 2. Occupation numbers for the reference configurations used in the CCI calculations

$^5B_2$ state										
Orbitals symmetry	C–Cσ a_1	C–Cσ* b_2	C–Cπ a_1	C–Cπ* b_2	3$d\sigma$ a_1	3$d\pi$ b_2	3$d\pi$ b_1	3$d\delta$ a_1	3$d\delta$ a_2	4s a_1
1	2	0	2	0	2	2	1	1	1	1
2	2	0	0	2	2	2	1	1	1	1
3	2	0	2	1	2	1	1	1	1	1
4	2	0	2	2	2	0	1	1	1	1
$^3B_2$ state										
Orbitals symmetry	C–Cσ a_1	C–Cσ* b_2	C–Cπ a_1	C–Cπ* b_2	3$d\sigma$ a_1	3$d\pi$ b_2	3$d\pi$ b_1	3$d\delta$ a_1	3$d\delta$ a_2	4s a_1
1	2	0	2	0	2	2	1	0	1	2
2	2	0	2	0	2	2	1	2	1	0
3	2	0	2	0	2	2	1	1	1	1
4	2	0	0	2	2	2	1	0	1	2
5	2	0	0	2	2	2	1	2	1	0
6	2	0	0	2	2	2	1	1	1	1
7	2	0	2	1	2	1	1	0	1	2
8	2	0	2	1	2	1	1	2	1	0
9	2	0	2	1	2	1	1	1	1	1
10	2	0	2	2	2	0	1	0	1	2
11	2	0	2	2	2	0	1	2	1	0
12	2	0	2	2	2	0	1	1	1	1

complex. Only the $^{3,5}B_2$ states were, however, studied in detail, since they are the only states where the donating iron orbital, $3d_{xz}$, is doubly occupied in the pure atomic states. In the B_1 and A_2 symmetries, the pure $^{3,5}F(d^7s)$ states are mixtures of two CSFs, with a weight of 80% for a CSF where $3d_{xz}$ is doubly occupied, and 20% for a CSF with $3d_{xz}$ singly occupied. The CSF of A_1 symmetry has $3d_{xz}$ singly occupied. Consequently, the geometry optimization was only performed for the $^{3,5}B_2$ states. The $^{3,5}B_1$ and $^{3,5}A_2$ states were examined at the equilibrium geometry of the $^{3,5}B_2$ states, and were found to have higher energies.

The geometry was optimized for the π-bonded form by independently varying the iron–carbon distance and a distortion parameter for the ethylene molecule. The distortion is described by a C–C stretch coordinate coupled to the bending angle for the CH_2 group: the angle between the C–C axis and the bisector of the H–C–H angle are coupled linearly, according to experience gained in the earlier work on the di-nickel ethylene complex [20].

Two different atomic states give potential curves of $^5B_2$ symmetry, namely $^5D(d^6s^2)$, resulting in a repulsive curve, and $^5F(d^7s)$, which gives an attractive curve. The CASSCF method cannot properly describe the avoided crossing between these two potential curves since the optimal orbitals are very different in the two states. Thus optimization of one state results in a very high energy for

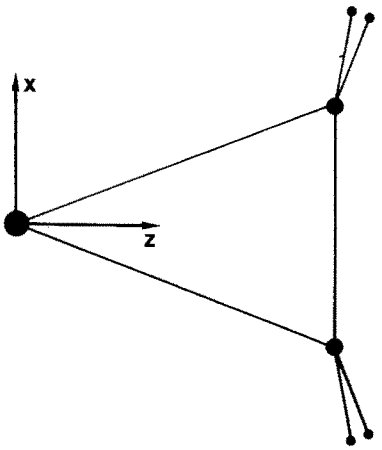

Fig. 1. Geometry and coordinate system for the π bonded structure of FeC_2H_4

the other and vice versa. The contracted CI calculation provides no remedy for this problem. The transition state was therefore estimated by computing the potential surface for the two states and locating the intersection with the lowest energy.

A brief examination of other geometric arrangements was made in order to discover the hydrogen-bonded structure postulated by Kafafi et al. This study also included an estimate of the dispersion interaction between iron in its ground state and ethylene (*vide supra*).

3. Results

3.1. The π-bonded structure

The potential curves obtained for the two $^5B_2$ states and the $^3B_2$ state are shown in Fig. 2. The lowest of the quintet state potentials goes asymptotically to the ground state of the iron atom; it is repulsive due to the interaction between the

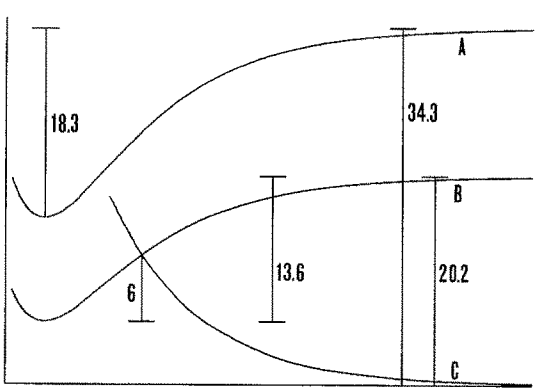

Fig. 2. Schematic potential curves for the three states studied. Energies are given in kcal/mol. *A*: $^3B_2$ state arising from the $^3F(d^7s)$ atomic state of iron. *B*: $^5B_2$ state arising from the $^5F(d^7s)$ atomic state of iron. *C*: $^5B_2$ state arising from the $^5D(d^6s^2)$ atomic state of iron

spatially extended and doubly occupied $4s$ orbital on iron and the π shell of ethylene. The $^5F(d^7s)$ state on the other hand shows an attractive interaction with ethylene. The same is true for the triplet potential curve, for which the singly occupied $4s$ orbital is hybridized away from ethylene by mixing with the $4p_z$ orbital, thereby decreasing the repulsion. Also, the other sp hybrid, which is empty and points towards ethylene, can act as an electron acceptor orbital. This sp hybridization leads to an unshielding of the $3d$ orbitals, and back donation can take place from $3d_{xz}$ to the ethylene π^* orbital. Thus the bonding mechanism follows closely the DCD model for both the high and low spin d^7s states.

The geometry for the two bound states was optimized by computing a grid in two dimensions and performing a polynomial fit. The two parameters used were the iron–carbon distance, and a distorsion coordinate describing the transformation of ethylene into a cyclopropane fragment. This distortion was achieved by varying the C–C distance, and at the same time bending the CH_2 groups away from the iron; these two parameters were coupled linearly as described in [20] but with the difference that the H–C–H angle was kept fixed at the ethylene value, 117.8°, for all geometries. The computed geometries are shown in Table 3. The similarity of the geometries found in the two different states indicates that the bonding mechanism is the same for both cases. Thus, in contrast to the situation in the corresponding nickel compound, the sd hybridization does not seem to be very important in the iron–ethylene complex. This difference between nickel and iron will be further analysed later.

The computed binding energy for the $^5B_2$ state arising from the d^7s asymptote is 10.7 kcal/mol at the CASSCF level of theory. Including dynamic correlation through the CCI calculations increases the value to 11.5 kcal/mol. A further increase to 13.6 kcal/mol is obtained by adding cluster effects through a multi-reference analogue of Davidson correction [24, 25]. This value is still 6.6 kcal/mol above the ground state asymptote, and the barrier to dissociation of the metastable state being estimated to be about 6 kcal/mol. These results were obtained using the large basis set (cf. Table 4).

The low spin state $^3B_2$ is very similar to $^5B_2$. Here the estimated binding energies at the CASSCF, CCI, and CCI + Davidson correction levels are 13.8, 16.0 and 18.3 kcal/mol, respectively. This is the lowest triplet state and no curve crossing occurs. Correlated energies for the triplet state have been estimated from

Table 3. The optimal geometry for the $^5B_2$ and $^3B_2$ states of $Fe(C_2H_4)$[a]

	R(Fe–C)	R(C–C)	∡ CCH_2[b]
Asymptotic limit	∞	1.35 Å	180.0°
Eq. $^5B_2$	2.12 Å	1.42 Å	198.4°
Eq. $^3B_2$	2.11 Å	1.42 Å	199.4°

[a] Obtained at the CCI level of theory

[b] The angle between C–C axis and the bisector of the angle ∡ HCH

Table 4. Binding energies for the d^7s $^5B_2$ and $^3B_2$ states of $Fe(C_2H_4)$ (in kcal/mol)[a]

	CASSCF	CCI	CCI + Q[b]
$^5B_2$ small basis	10.4	16.0	18.2
large basis	10.7 (0.3)[c]	11.5	13.6
$^3B_2$ small basis	13.1	20.1	22.5
large basis	13.8 (6.6)[c]	(16.0)[d]	(18.3)[d]

[a] With respect to the d^7s asymptotes
[b] With Davidson correction added
[c] Values in parentheses are obtained with the $4p$ orbital deleted from the basis set. Computed at the optimal geometries obtained with the full basis
[d] Estimated from the other basis set and correlation effects

small basis set calculations, adding the basis set effect obtained for the quintet state. This basis set effect is virtually zero at the CASSCF level, but has a profound effect on the dynamic correlation energies due to the lack of f-type functions in the small basis. This is not very surprising, considering that iron looses 0.7 d-electrons in going from the asymptotic d^7s configuration to the equilibrium structure. As a result the computed binding energy decreases when f-type functions are added to the basis set. Further improvement in the description of the $3d$ shell correlation can be expected to decrease the binding energy slightly more. On the other hand, an enhanced binding is expected from the correlation of the remaining σ electrons on ethylene. The effect has not been studied explicitly here, but a comparison to a recent study of NiCO is illustrative [26]. Correlation of the electrons on CO directly involved in the bonding to Ni (the σ lone-pair and the π electrons) resulted in a binding energy of 27 kcal/mol, which increased to 33 kcal/mol when the remaining valence electrons were also correlated. A similar, but smaller, effect can be expected in the complex studied here. The effect of missing electron correlation in the $3d$ shell and in the ethylene moiety are thus of opposite sign. We therefore believe the present results to be close to the basis set limit. A compilation of the computed energies can be found in Table 4.

The other states of potential interest, the $^{3,5}B_1$ and $^{3,5}A_2$ states, were examined at the equilibrium geometry found for the B_2 states. $^5B_1$ was found to be very close in energy to $^5B_2$, being 1 kcal/mol higher, while $^5A_2$ was found to be 5 kcal/mol above the $^5B_2$ state. The $^3B_1$ state is virtually degenerate with $^3B_2$, and $^3A_2$ lies 1 kcal/mol higher. The bonding mechanism for these states in the other symmetries is the same as in $^{3,5}B_2$, and they will not be examined further.

3.2. Structures with iron bonded to the hydrogen atoms

The results for the π complex shows that the ground state potential curve is repulsive. The iron atom can therefore be only weakly bound to ethylene in this

configuration, through dispersion interactions. If this is the case, the π-bonded structure does not necessarily represent the lowest energy for the complex. Kafafi et al. [11, 12] have actually given evidence for alternative structures in which the iron atom is bonded to one or two of the hydrogen atoms in ethylene. Two of these possible structures are shown below:

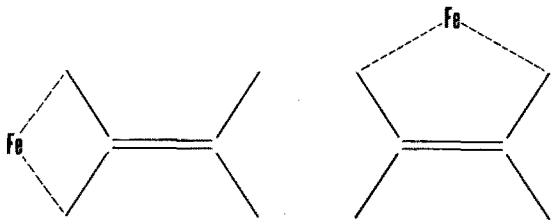

1 2

A theoretical estimate for the binding energies in these structures is not easy, since the dominant mechanism is a dispersion interaction between Fe d^6s^2 and ethylene. We have nevertheless made a preliminary study of the potential by calculating the CASSCF energy as a function of the distance of the iron from the alkene; the active space used consisted of the iron $3d$ and $4s$ electrons. The wave function for this active space is represented by a single open shell SCF configuration. The ethylene geometry was kept fixed at its asymptotic structure.

The potential curves for both (1) and (2) were found to be repulsive at this level of theory. This is not unexpected, since the only binding mechanism which would work in the SCF approximation arises from weak permanent and induced electrostatic interactions, with the first non-vanishing term being the quadrupole-quadrupole interaction.

An *ab initio* calculation of the dispersion interaction is not possible for a molecule of the present size. The dispersion forces were therefore estimated using a simplified model, where the ethylene molecule is described as an assembly of anisotropic point polarizabilities. The London formula is then used to calculate the interaction energy as a function of the iron–ethylene distance [21, 22].

These calculations result in a binding energy of around 0.5 kcal/mol for all the three structures (the π-bonded conformation and (1) and (2)). The iron–carbon distances were 4.2, 4.5, and 4.5 Å, respectively. It is likely that the method used underestimates the interaction energy in this case, since no geometry optimization has been performed and since effects from intra-molecular correlation have not been included. It is clear, however, that the iron will be only very weakly bound to ethylene in its ground state, and that different bonding sites will have similar binding energies.

4. Discussion

The high spin state in nickel ethylene is only weakly bound. No bonding was actually found in our earlier work on that system, but that was due to an

incomplete search of the potential surface for longer Ni–C distances [2]. The corresponding nickel–acetylene complex was found to be bound with around 1 kcal/mol [5]. Population analysis showed a considerable population of the $4p_z$ orbital in both these complexes leading to the formation of two *sp* hybrids. The one pointing away from the nickel–carbon bond unshields the nickel $3d$ shell and opens the route to back bonding. The other hybrid orbital forms a weak bond with the π shell of the C–C bond. For nickel, this hybridization leads only to weak bonding. The excitation energy to the d^9p configuration is also large (81 kcal/mol).

On the other hand, the high spin d^7s complex between iron and ethylene is bound with more than 10 kcal/mol. We can expect the same mechanism to be operating as for the nickel atom. The excitation energy $^5F(d^7s)$ to $^5D(d^7p)$ is 76 kcal/mol, which is not very different from nickel, and the degree of *sp* hybridization is therefore the same in both systems. The important difference between the two atoms lies in the donating power of the $3d$ electrons, which is much larger in iron than in nickel. The $3d$ ionization energy is smaller, and the size of the $3d$ orbital is more comparable to the $4s$. Thus $3d$ is more easily unshielded in iron. The population analysis (cf. Table 5) also shows a considerably larger back donation of electrons from $3d_{xz}$ to ethylene in iron than in nickel—0.7 electrons compared with only 0.2 electrons in NiC_2H_4, $^3A_1$.

In order to investigate more closely the importance of the *sp* hybridization effect on the bonding we have repeated the CASSCF calculation at the equilibrium geometry, but with only two *p*-type orbitals in the basis set for iron ($2p$ and $3p$); the $4p$ orbital is thus absent. Such a calculation is especially easy to do with basis functions of the ANO type, since each function corresponds to an

Table 5. Mulliken population analysis for the d^7s $^3B_2$ and $^5B_2$ states of FeC_2H_4[a]

Fe	AL(d^7s)	Large basis		Small basis			
		$^5B_2$	$^3B_2$	$^5B_2$	$^5B_2$[c]	$^3B_2$	$^3B_2$[c]
$3d(a_1)$[b]	3.00	3.02	3.03	3.01	(3.01)	3.02	(3.01)
$3d_{xz}(b_2)$	2.00	1.27	1.29	1.27	(1.29)	1.29	(1.31)
$3d_{yz}(b_1)$	1.00	1.01	1.01	1.01	(1.00)	1.01	(1.00)
$3d_{xy}(a_2)$	1.00	1.00	1.00	1.00	(1.00)	1.00	(1.00)
$4s(a_1)$	1.00	1.00	1.07	0.95	(1.28)	1.01	(1.33)
$4p_z(a_1)$	0.00	0.47	0.41	0.46	(–)	0.41	(–)
$4p_x(b_2)$	0.00	0.05	0.04	0.05	(–)	0.05	(–)
$4p_y(b_1)$	0.00	0.01	0.01	0.01	(–)	0.01	(–)
C (all)	6.21	6.32	6.31	6.37	(6.49)	6.35	(6.46)
H (all)	0.89	0.88	0.88	0.88	(0.86)	0.87	(0.85)
C_2H_4 (charge)	0.00	−0.17	−0.13	−0.24	(−0.42)	−0.21	(−0.34)

[a] Gross atomic populations at the asymptotic limit (AL) and at the equilibrium geometries (CASSCF results)

[b] Sum of $3d_{y^2-x^2-z^2}$ and $3d_{x^2-z^2}$

[c] Without $4p$ on Fe

orbital for the free atom. The calculated binding energy is decreased by 10.4 kcal/mol to 0.3 kcal/mol. Thus almost all binding disappears, although the donation of electrons from $3d_{xz}$ is hardly affected (0.71 electrons instead of 0.73, cf. Table 5). The $3d$ orbital maintains its donating power even when no unshielding of the $4s$ electron takes place. Note that the ethylene fragment is highly distorted also in this case. There is thus more binding energy in the back donation process than is evident from the small binding energy.

As can be seen from Table 5 there is a large population of the $4p_z$ orbital. With this orbital deleted from the basis set, the $4s$ orbital increases its population (from 1.0 to 1.3 electrons); however it is difficult to draw any conclusions from these numbers, since both these orbitals have their maxima at the same place as the π orbital of the ethylene moiety. For the same reason, not much meaning can be attached to the computed gross atomic charges given in the table.

The features of the bonding analysed above for the high spin d^7s complex between iron and ethylene are independent of the spin coupling, and therefore should be equally important in the low spin $^3B_2$ state. This is also clear from the population analysis, which shows the same amount of charge transfer from $3d$ in both cases. The calculation without the $4p$ orbital was also performed in this case, resulting in a lowering of the binding energy from 13.8 kcal/mol to 6.6 kcal/mol. The difference is somewhat smaller here, probably due to the *sd* hybridization which now can compete with the *sp* effect. The *sd* hybridization in the corresponding nickel complex was found to be the major characteristic of the bonding mechanism. However, its importance must be considerably smaller for iron since it involves an excitation from d^7s to d^8, with an excitation energy of around 60 kcal/mol. The corresponding d^9s to d^{10} energy difference in nickel is only around 30 kcal/mol. Occupation numbers for the two *sd* hybrids are also much closer to one in the iron complex: 1.2 and 0.8, respectively. The corresponding number in the nickel complex is 1.8 and 0.2. However, the difference increases when the $4p$ orbital is deleted from the basis set: 1.3 and 0.7. Thus, to some extent, *sd* hybridization through the $4p$ orbital, which explains the smaller decrease in binding energy in the low spin case when $4p$ is deleted.

To summarize: the d^7s π complex between iron and ethylene shows very similar binding features, independent of the spin coupling of the $3d$ electrons. The low spin form has a somewhat larger binding energy due to the possibility of *sd* hybridization, but the major source of binding is the back donation of electrons from the $3d$ shell of iron to the π^* orbital on ethylene. This is facilitated by hybridization between the $4s$ and $4p$ orbitals, which also gives rise to some transfer of electrons to iron through interaction with the π orbital. It should, however, be remembered that both these states represent excited potential surfaces: the ground state surface is only bound through dispersion forces.

5. Conclusions

The present investigation of the complex formation between an iron atom and ethylene has resulted in the negative conclusion that no chemical bond is formed

between the two moieties in their ground electronic states. The interaction is characterized by dispersion forces and the binding energy can be expected to be small. No preferred binding site was found for the iron atom. This result is not necessarily in conflict with the photochemical process leading to insertion of iron into the C–H bond, found by Kafafi et al. [11]. The excitation is most probably to Fe d^6sp, corresponding to a wave length of 370 nm. The photolysis was performed in the near UV wave lengths slightly smaller (280–360 nm). Iron in this configuration is very reactive and will easily break the C–H bond, independently of where it is originally located, as long as the distance to ethylene is not too large.

The bonding in the excited states corresponding to the d^7s asymptote has been analysed in terms of *sp* and *sd* hybridization and shows that the main mechanism is through back donation of electrons from 3*d* to ethylene. A detailed analysis of the bonding mechanism in FeCO using the constrained space orbital variation method [6] showed a structure very similar to the one obtained in the present work. The results can therefore be expected to have a general validity for the description of chemical bonds of this type. It should be emphasized that even if the d^7s potential surface is not the lowest for the naked Fe complex, it is stabilized by the presence of other ligands, like CO. It also most probably represents the ground state when more than one ethylene molecule is bound to iron. The di-ethylene complex of nickel has been studied by Siegbahn and Brandemark [23]. They showed that the most stable form was obtained with the two ethylene moieties bound at right angles to each other (D_{2d} symmetry). The reason is that such a structure makes it possible to form two simultaneous $3d\pi$ bonds. A similar situation can be expected to occur in $Fe(C_2H_4)_2$, which then explains why these complexes are more easily formed in the cryogenic matrices than the monomer complex.

Acknowledgements. We thank docent Gunnar Karlström and Dr. Anders Wallqvist for help with the calculation of the dispersion forces. The research reported in this communication has been supported by a grant from the Swedish Natural Science Research Council (NFR) and by IBM Sweden under a joint study contract.

References

1. Rives AB, Fenske RF (1981) J Chem Phys 75:1293
2. Widmark P-O, Roos BO, Siegbahn PEM (1985) J Phys Chem 89:2180
3. Siegbahn PEM, Blomberg MRA (1984) Chem Phys 87:189
4. Bauschlicher Jr, CW (1985) Chem Phys Letters 115:387
5. Widmark P-O, Sexton GJ, Roos BO (1986) J Mol Struct (Theochem) 135:235
6. Bauschlicher Jr, CW, Bagus PS, Nelin CJ, Roos BO (1986) J Chem Phys 85:354
7. Bauschlicher Jr, CW, Pettersson LGM, Siegbahn PEM (1987) J Chem Phys 87:2129
8. Barbier C, Berthier G, Daoudi A, Suard M (1988) Theor Chim Acta 73:419
9. Chatt J, Duncanson LA (1953) J Chem Soc 2939; Dewar MJS (1951) Bull Soc Chim Fr 79
10. Parker SF, Peden CHF, Barrett PH, Pearson RG (1983) Inorg Chem 22:2813
11. Kafafi ZH, Hauge RH, Margrave JL (1985) J Am Chem Soc 107:7550
12. Kline ES, Kafafi ZH, Hauge RH, Margrave JL (1985) J Am Chem Soc 107:7559
13. Almlöf J, Taylor PR (1987) J Chem Phys 86:4070

14. Wachters AJH (1970) J Chem Phys 52:1033
15. Ahlrichs R, Scharf P, Ehrhardt C (1985) J Chem Phys 82:890
16. van Duijneveldt FB (1970) IBM Technical Research Report RJ945
17. Roos BO, Taylor PR, Siegbahn PEM (1980) Chem Phys 48:157; Roos BO (1980) Int J Quantum Chem S14:175
18. Roos BO (1987) Adv Chem Phys LXIX, *Ab initio* methods in quantum chemistry, part II, p 399.
19. Siegbahn PEM (1981) In: Carbo R (ed) Current aspects of quantum chemistry. Proceedings of the International Congress, Barcelona, Spain 1981, Elsevier, Amsterdam
20. Widmark P-O, Roos BO (1987) Theor Chim Acta 71:411
21. Karlström G (1982) Theor Chim Acta 60:535
22. Karlström G, Wallqvist A: private communication
23. Siegbahn PEM, Brandemark UB (1986) Theor Chim Acta 69:119
24. Davidson ER (1974) In: Daudel R, Pullman B (eds) The world of quantum chemistry. Reidel, Dordrecht
25. Blomberg MRA, Siegbahn PEM (1983) J Chem Phys 78:5682
26. Blomberg M, Brandemark U, Johansson J, Siegbahn P, Wennerberg J (1988) J Chem Phys 88:4324